Polarization effects in the excitation and emission of Fe^{3+} in orthoclase and their relevance to the determination of lattice sites of unknown defects

2005 J. Phys.: Condens. Matter 17 205

(http://iopscience.iop.org/0953-8984/17/1/019)

INSTITUTE OF PHYSICS PUBLISHING JOURNAL OF PHYSICS: CONDENSED MATTER

J. Phys.: Condens. Matter **17** (2005) 205–220 doi:10.1088/0953-8984/17/1/019

Polarization effects in the excitation and emission of Fe^{3+} in orthoclase and their relevance to the determination of lattice sites of unknown defects

M A Short

Department of Physics, Simon Fraser University, Burnaby, BC, Canada

E-mail: mashort@sfu.ca

Received 30 July 2004, in final form 22 November 2004
Published 10 December 2004
Online at stacks.iop.org/JPhysCM/17/205

Abstract

A method was recently proposed for determining possible lattice sites of an unknown defect from polarization effects in its optical transitions. In this paper the method is tested using the optically excited 1.77 eV (700 nm) fluorescence of Fe^{3+} ions which predominantly occupy the T1 sites in orthoclase feldspar. The emission intensity depended on the polarization of the exciting photons and the emission was itself polarized. Two pairs of crystal field symmetry directions were deduced from polarization data for each of the transitions at 1.77, 2.79 and 3.26 eV, and one pair was aligned with symmetry axes in the average geometry of the four anions around the T1 sites. An analysis of EPR data for Fe^{3+} ions in feldspar showed that there was a symmetry axis in the crystal field similar to one of those deduced from the polarization data. Group theory calculations were used to determine if the transitions were dipolar—a major assumption of the method. Three symmetries (S_4, C_{2v} and C_2) were found to lead to dipolar transitions consistent with the excitation results, and four (D_2, C_3, C_2 and C_s) were consistent with a 1.77 eV dipolar emission.

1. Introduction

Short (2004) proposed a method for determining the possible lattice sites of an unknown defect in orthoclase from the polarization effects in the optical transitions of the defect. The method works by predicting a symmetry direction of the crystal field around the defect and then comparing this prediction with the symmetry, or approximate symmetry, directions of the average crystal structure. The average crystal structure does not have to have an actual symmetry axis that matches the prediction, because it was assumed that the geometry around a defect can be slightly distorted from the average. Support for the validity of the method would be obtained if it could correctly predict the lattice sites of a known defect in orthoclase from

the polarization effects in the optical transitions of the defect. Here it shall be shown that this supporting information was obtained from optical transitions in Fe^{3+} ions.

Orthoclase is a type of feldspar in which iron is a well known impurity predominantly substituting for Al^{3+} cations in T1 sites (see e.g. Smith and Brown 1988, Nadezhina *et al* 1993). The impurity has been associated, on the basis of theoretical calculations and abundance, with a 1.77 eV emission obtained with a variety of excitation methods (see e.g. Geake *et al* 1973, Kirsh and Townsend 1988). Short (2003, figure 6.1) found that an irradiated orthoclase crystal (K3) had a phosphorescence at or near 1.77 eV with polarization effects similar to those of the 1.45 eV-excited, 3.1 eV emission of the same sample (Short 2004). The most likely explanation for the phosphorescence was transitions in Fe^{3+} ions in T1 sites, and thus this emission presented an opportunity to test the method of determining the lattice sites of the ions from the polarization effects.

If the phosphorescence intensity (I) is due to dipolar transitions in Fe^{3+} ions, I is predicted (by an equation first given by Short and Huntley (2000)) to vary with φ and θ as

$$I \propto \cos^2(\varphi)\cos^2(\theta) + \sin^2(\varphi)\sin^2(\theta) \tag{1}$$

where φ is the angle a projection of the dipoles in a plane normal to the photon propagation direction makes with one of the principal directions lying in that plane, and θ is the angle the transmission axis of an external polarizer makes with the same principal direction. Equation (1) was fitted to the 1.77 eV phosphorescence data $I(\theta)$ of one crystal slice, where it was found to account for the variation in intensity very well by solving for φ. This fitting procedure was repeated for data obtained from two additional slices of a crystal which were not parallel to each other or the first slice. Two pairs of dipole directions were deduced from the φ values. Encouragingly, one pair of dipole directions was aligned nearly parallel with two approximate symmetry axes in the average geometry of the four anions around the T1 sites (they were off by 14.5° and 11.5° respectively). Thus it would appear that this initial test of the method on a known ion occupying known sites was successful in predicting their site location.

However, there were some weak aspects to the test that needed clarification. First, although two elemental analyses (inductively coupled plasma mass spectrometry and x-ray fluorescence) did determine that there were trace amounts of iron in K3, there was still some doubt as to whether the 1.77 eV phosphorescence was coming from Fe^{3+} ions or not. Second, although one can deduce from x-ray diffraction data that the geometry of the four anions around the Fe^{3+} ions in T1 sites is not very different from the average geometry for T1 sites (see Nadezhina *et al* 1993, Short 2003), the precise geometry is not known. One must assume that the geometry has a symmetry axis that coincides with one of the dipole directions deduced from the polarization data. Third, even if such a anion geometry exists, it is not known if this could actually cause the occurrence of a dipolar 1.77 eV transition with an associated dipole direction consistent with one of those deduced from the data.

An experiment that can provide useful information on the origin of the 1.77 eV phosphorescence is an optically excited 1.77 eV fluorescence measurement. That the emission is from Fe^{3+} ions in T1 sites can be determined by making use of the characteristic optical excitation spectrum that uniquely identifies it (Telfer and Walker 1978). Optically excited fluorescence is a sensitive technique, and it is therefore particularly suited for detecting trace amounts of an impurity ion (Telfer and Walker 1975). Furthermore, since the optical excitation and the fluorescence are due to optical transitions in the same ions, the polarization effects in all the transitions should (assuming they are dipolar) be consistent with Fe^{3+} ions in T1 sites.

An experiment that can provide information on the symmetry of the crystal field around Fe^{3+} ions is electron paramagnetic resonance (EPR). This is possible because Fe^{3+} ions are paramagnetic, and maxima and minima in the magnitude of the EPR g tensor will occur for

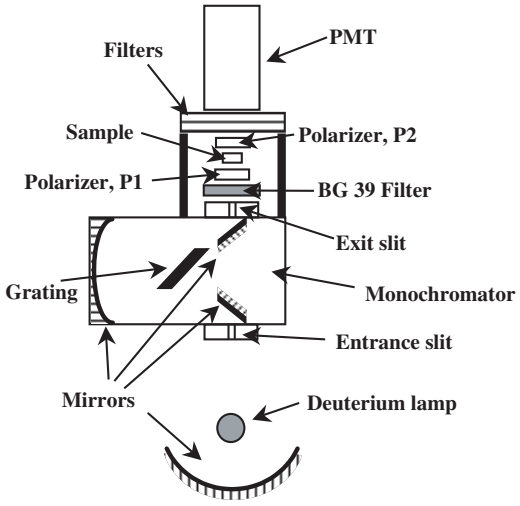

Figure 1. Schematic diagram of the equipment used to measure optically excited fluorescence (not to scale). For measuring unpolarized fluorescence, no polarizers were used. For polarized excitation, only the lower polarizer (P1) was used, and for measuring the polarization of the emitted fluorescence, only the upper polarizer (P2) was used.

non-cubic crystal fields. Furthermore, the direction of the external magnetic field at which the maxima and minima occur will align with symmetry axes of the crystal field (Marfunin 1979, p 94). Thus one can determine if the symmetry directions deduced from the EPR data are consistent with those deduced from the polarization data.

Finally, since the optical transitions in Fe^{3+} ions are well understood (see e.g. White *et al* 1986), one can use group theory (see e.g. Cotton 1990) to determine if any of the transitions in the free ion, modified by the crystal field, are indeed dipolar with a dipole direction consistent with those predicted from the polarization and EPR data.

Thus the fluorescence measurements were carried out, the EPR data from feldspars presented by others was analysed, and whether a transition was dipolar or not was calculated using group theory.

2. Experimental details

A brief description of the equipment used to measure the polarization effects in the optically excited fluorescence is given here; further details can be found in Short (2003 and 2004). A diagram of the experimental set-up is shown in figure 1. Photons with energies between 1.77 and 6.2 eV (700 and 200 nm) from a Jarrell-Ash[1] 45-541A deuterium lamp were focused onto the entrance slit of a Jarrell-Ash 82-410 monochromator using a concave mirror. The output photon energy from the monochromator was changed by rotating the grating with a computer controlled stepper motor. Large slit widths ($\approx$0.5 mm) were used to allow a sufficient number of photons to excite a sample so that fluorescence photon counting statistics were optimal without sacrificing energy resolution too much. With these widths, the estimated resolution in the excitation spectrum ranged from about 0.006 eV at 1.77 eV to about 0.1 eV at 6.2 eV (i.e. 2–3 nm, from manufacturer's data). A Schott BG 39 filter (3 mm thick) over the exit slit was used to absorb scattered and second-order diffracted photons.

Fluorescence and scattered light were measured with an EMI 9558QB (red sensitive) photomultiplier tube (PMT), cooled to $-30\,^{\circ}$C. The solid angle subtended from the sample to

[1] Jarrell-Ash Company, 590 Lincoln Street, Waltham, MA, USA.

the PMT photocathode was about 0.1 sr. To make sure only photons with energies at, or near, 1.77 eV were predominant, filters were placed between the sample and the photocathode. The best combination was found to be two narrow bandpass interference filters, type 700/40/75[Note 2] each having a peak transmission of 75% at 1.77 eV and an FWHM of 0.1 eV (40 nm). These interference filters emitted considerable red fluorescence when exposed to photons with energies outside their pass band; this fluorescence was reduced to negligible levels by including both a Kopp 4-77 bandpass filter and a Schott KV 550 low fluorescence filter (3 mm thick) between the sample and the interference filters.

The orthoclase feldspar chosen for the fluorescence measurements was the same as the one (K3) used for phosphorescence measurements (see Short 2003), and the 1.45 eV-excited, 3.1 eV luminescence measurements (see Short 2004). Slices ≈1.5 mm thick and large enough to cover the whole exit slit of the monochromator (≈0.5 mm × 10 mm) were cut from larger crystals so that the two largest surfaces of each slice were parallel to (0 0 1) and (0 1 0). One naturally occurring slice, approximately 3 mm thick, and with two large surfaces parallel to $(\bar{2}\ 1\ 1)$, was also used. These slices were called A, E and D respectively. The slices were polished using 600 grade carborundum paper, and then 1.0 μm polishing powder. The principal directions of the refractive index were determined for slices A and E by optical microscopy, and two were found to lie in the plane of each slice (within a few degrees). However, no principal directions were found to lie in the plane of slice D; this was consistent with the diagram given by Deer *et al* (1992, figure 144).

For measurements using unpolarized optical excitation, a polished slice was placed close to the exit slit of the monochromator, above the blocking filter if one was required. For measurements using polarized excitation, an Oriel 27341 dichroic polarizer (P1 in figure 1) was placed in the light path between the exit slit and a sample slice. The polarizer could be manually rotated relative to the sample slice. A scale was marked on the circumference of a fixed concentric ring housing the polarizer so the angular position (ζ) of the transmission axis relative to the ring could be measured. After completion of a measurement the relation between the fixed ring and a principal direction of the sample slice was determined. A similar procedure was used to measure the polarization of the emitted fluorescence, except another dichroic polarizer (P2), Oriel 27341, was used and this was placed between the sample slice and the PMT filters.

Background counts were recorded using the different experimental arrangements without any sample slice; these background counts were subtracted from the fluorescence photon counts from a sample slice. The fluorescence intensity was also corrected for the variation of intensity with photon energy of the excitation source as follows. The PMT filters were replaced with neutral density filters, and the spectrum of the excitation source measured without any sample slice, but with a blocking filter if required for the different energy ranges. Spectra were obtained both with and without the polarizer (P1). These spectra were corrected for the energy dependence of the neutral density filters, and for the PMT photocathode sensitivity (manufacturer's data), and then used to correct the 1.77 eV fluorescence intensity obtained at different photon excitation energies.

3. Results

3.1. Excitation spectra, measuring unpolarized emission

In figure 2, polarized and unpolarized excitation spectra are shown whilst measuring the 1.77 eV fluorescence. The figure shows two spectra for slice A and two spectra for slice

[2] Intor Inc., 1445 Frontage Road, NW Socorro, NM 87801, USA.

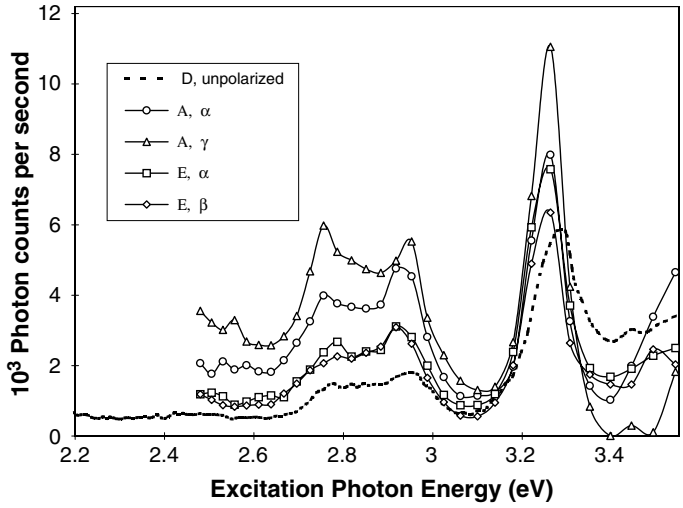

Figure 2. Change in the 1.77 eV fluorescence intensity with photon energy and polarization of the exciting light. Low fluorescence intensity prevented the accurate measurement of spectra outside the energy range shown. The spectra obtained with unpolarized excitation were similar for all slices, thus only data for slice D are shown. For polarized excitation, slice D gave a similar response to slice A, and thus the data for it are not shown for clarity. α, β and γ are the principal directions. The data for slices A and E have been scaled up by factors of 6 and 2 respectively for clarity. Uncertainties due to photon counting statistics are contained within the symbols.

E; these correspond to polarized excitation when the direction of the transmission axis of P1 was aligned (within experimental error) to the two principal directions that lie in plane of each slice. All the spectra in figure 2 have three prominent excitation peaks occurring near 2.79, 2.92 and 3.26 eV, and a number of minor peaks.

The relative change in the emission intensity between the two spectra of slices A and E shown in figure 2 clearly depended on the energy of the exciting photons, and this dependence appears to be similar for both slices. Figure 3 shows this effect; slice D data (not shown) were similar to those of slice A. Note that the maxima and minima with 2.92 eV excitation did not occur when the polarizer was aligned with the principal directions of the sample slices.

3.2. Excitation spectra, measuring polarized emission

Figure 4 shows excitation spectra using unpolarized excitation and measurement of the 1.77 eV fluorescence with the emission polarizer (P2). The figure shows two spectra for slice A and two spectra for slice E; these are for measurement of the emission when the transmission axis of P2 was aligned close to the principal directions that lie in the plane of each slice.

The relative change in the emission intensity between the two spectra of a slice shown in figure 4 appeared to be only weakly dependent on the energy of the exciting photons, but the magnitude of the change depended on which slice was measured. Figure 5 shows this effect for each prominent excitation peak for slices A and E. Slice D data (not shown) were similar to those of slice A.

4. Dipole directions and the crystal structure

Dipole directions were deduced from the $\pm\varphi$ values of slices A (0 0 1) and E (0 1 0) given in table 1. For polarized excitation at 3.26 eV, the directions of the dipoles were in two pairs

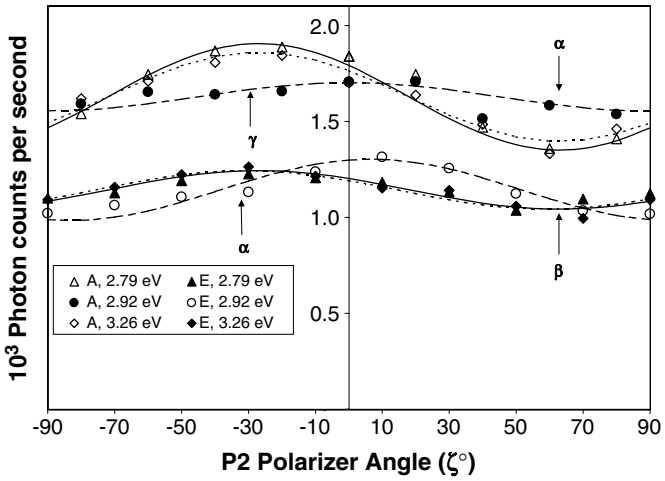

Figure 3. Change in the 1.77 eV fluorescence intensity of slices A and E as the polarizer (P1) was rotated below the sample being excited with 2.79, 2.92, and 3.26 eV photons. The polarizer angle ζ was relative to a fixed ring holding the sample. α, β and γ are the principal directions. The data for each slice have been normalized to the average emission intensity obtained with 3.26 eV excitation, and all the data from slice E were scaled by 0.3 for clarity. The estimated uncertainties are contained within the symbols; the uncertainties in the intensities are larger than that shown in figure 2 because of the uncertainty in producing the same excitation energy for each data point in a series. The solid, dashed and dotted curves are fits, using equation (1), to the 2.79, 2.92 and 3.26 eV data respectively. The φ values obtained from the fits, along with those obtained from fits to the data of slice D, are listed in table 1.

consistent with the $C2/m$ group symmetry of orthoclase: [93 45 100] and [93 $\bar{4}5$ 100], and [$\bar{6}3$ 79 100] and [$\bar{6}3$ $\bar{7}9$ 100][Note 3]. The above directions were viewed together with the crystal structure using a 3D plotting program, and one pair was found to align close to approximate symmetry directions in the geometry of the four anions around the T1 sites in feldspars as shown in figure 6. The angles between the dipole directions and the approximate crystal symmetry directions (obtained from x-ray diffraction data) were calculated and are listed in table 2. The estimated experimental error is $\approx 3°$.

The dipole directions deduced from the data with 2.79 eV excitation were similar to those obtained with 3.26 eV excitation and thus they align with the crystal structure in a similar way. However, the dipole directions deduced from the 2.92 eV data were very different and did not appear to align with any obvious crystal symmetry axis.

The dipole directions deduced from the $\pm\varphi$ angles obtained from the fits to the fluorescence data (figure 5) also consisted of two pairs: [66 23 100] and [66 $\bar{2}3$ 100], and [$\bar{2}0$ 46 100] and [$\bar{2}0$ $\bar{4}6$ 100]. These dipole directions were also compared to the crystal structure using a 3D plotting program, and the same symmetry directions as those deduced from the 2.79 and 3.26 eV excitation data were found to be the best match for one dipole pair, although the alignment was not as good (see table 2). Furthermore, this same pair of dipoles was experimentally indistinguishable from those found for the 1.77 eV phosphorescence.

[3] For the data to be truly consistent with a dipolar transition requires the correct prediction for the alignment of the projection of the dipole onto the surface of a third slice after fixing the dipole orientation from the projections that the dipole would make on the surfaces of two other slices which are not cut parallel to the third or to each other. In this case the dipoles deduced from the data of slices A and E did not correctly predict the $\pm\varphi$ angles obtained for slice D. This was probably caused by the fact that principal directions did not lie in plane of the slice nor did the [0 1 0] axis—both are required (see Short 2004).

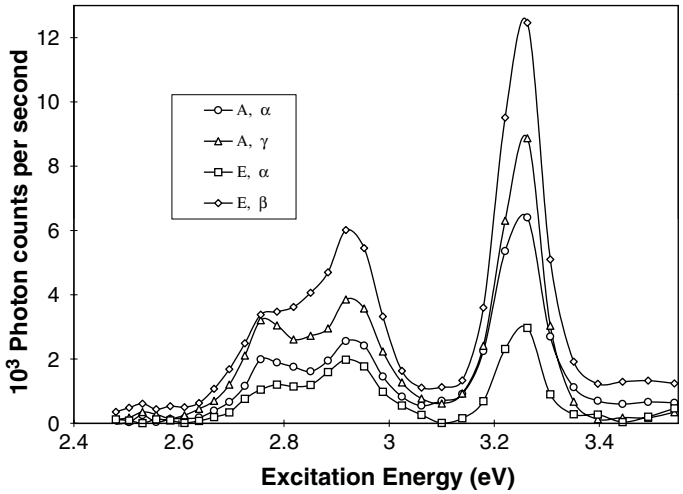

Figure 4. Change in the 1.77 eV fluorescence intensity with photon energy of the exciting light and polarization of the emission. Slice D gave a similar response to slice A and thus the data for it are not shown for clarity. α, β and γ are the principal directions. Uncertainties due to photon counting statistics are contained within the symbols.

Table 1. Summary of the polarization results with 1.77 eV emission. (Note that the first column describes five cases where the polarization of the photons was varied in fluorescence and phosphorescence experiments on K3 (the latter were reported in Short (2003) and are included here for easy comparison). The other columns describe how the number of emission photons changed for the different sample slices. e.g. columns 2–4 are the results for slice A, which is the (0 0 1) plane, and the emission or excitation was propagating in, or close to, the β direction. Column 2 is for photons polarized in the α direction and column 3 for photons polarized in the γ direction. The entries in these columns indicate whether the photon counts were at a maximum or a minimum with an estimated uncertainty of around $\pm 3°$. Column 4 is the $\pm\varphi$ angles obtained from fits to the data by equation (1); these are relative to the polarization direction of maximum photon counts.)

	Slice A (0 0 1), β[a]			Slice D ($\bar{2}$ 1 1), α[a]			Slice E (0 1 0), γ		
Fluorescence at 1.77 eV with	α[a]	γ	$\pm\varphi$	β[a]	γ[a]	$\pm\varphi$	α	β	$\pm\varphi$
polarized excitation at 2.79 eV	Min	Max	40°	Min	Max	41°	Max	Min	43°
polarized excitation at 2.92 eV	[b]	[b]	44°	[c]	[c]	45°	[b]	[b]	41°
polarized excitation at 3.26 eV	Min	Max	41°	Min	Max	43°	Max	Min	43°
Excitation at 2.79, 2.92 or 3.26 eV with	α[a]	γ	$\pm\varphi$	β[a]	γ[a]	$\pm\varphi$	α	β	$\pm\varphi$
polarized fluorescence at 1.77 eV	Min	Max	39°	Max	Min	40°	Min	Max	28°
Radiation induced phosphorescence with	α[a]	γ	$\pm\varphi$	β[a]	γ[a]	$\pm\varphi$	α	β	$\pm\varphi$
polarized emission at 1.77 eV	Min	Max	36°	Max	Min	41°	Min	Max	29°

[a] For slices A and D, the propagation and polarization directions were not aligned parallel with the principal directions in all cases, but were skewed about 8° and 18° from alignment respectively.
[b] The maximum and minimum intensities did not occur at the principal directions.
[c] Means that there was no clear maximum and minimum.

5. Discussion

Geake *et al* (1973 and 1977), Telfer and Walker (1975 and 1978), Marfunin (1979, p 197), Slaats *et al* (1991), Zink *et al* (1995) and Poolton *et al* (1996) all show excitation spectra using unpolarized excitation for 1.77 eV fluorescence emission in feldspars. Their data consistently showed a sharp peak near 3.26 eV and two overlapping peaks near 2.79 and 2.95 eV. There

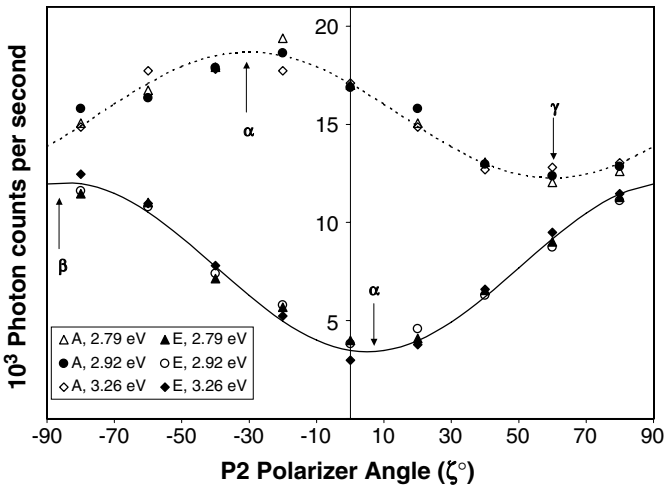

Figure 5. Change in the 1.77 eV fluorescence intensity of slices A and E as the polarizer P2 was rotated above the sample being excited with 2.79, 2.92, and 3.26 eV photons. The polarizer angle ζ was relative to a fixed ring holding the sample. α, β and γ are the principal directions. The variation in intensity of each peak was scaled so that the average intensity was the same as the average intensity obtained with 3.26 eV excitation, and all the data from slice A were scaled by an additional factor of 2 for clarity. The dotted and solid curves are fits using equation (1) to the combined data of the three prominent excitation peaks of slices A and E respectively. The φ values obtained from the fits, along with those obtained from the fit to the data of slice D, are listed in table 1. The estimated uncertainties are contained within the symbols.

Table 2. The angles between the deduced dipoles and certain crystal directions. (Note that the first column contains the vectors for pairs of dipole directions deduced from the $\pm\varphi$ angles of the fits to the fluorescence data for K3. Also shown in this table are the dipole directions deduced from the fits to the 1.77 eV phosphorescence (Short 2003). The headings of the next four columns are for different directions in the feldspar lattice calculated from x-ray diffraction data (Colville and Ribbe 1968). Each angle is the amount of deviation between a dipole and a crystal direction calculated from their dot product.)

	Crystal directions			
Dipole directions	$T1_o \longrightarrow OD_o$	$T1_m \longrightarrow OD_m$	$T1_m \longrightarrow (OB + O1)_m$	$T1_o \longrightarrow (OB + O1)_o$
Excitation at 3.26 eV	[94 32 100]	[94 $\bar{3}2$ 100]	[87 34 100]	[87 $\bar{3}4$ 100]
[93 45 100]	8.6°	—	7.1°	—
[93 $\bar{4}5$ 100]	—	8.6°	—	7.1°
Fluorescence at 1.77 eV	[94 32 100]	[94 $\bar{3}2$ 100]	[87 34 100]	[87 $\bar{3}4$ 100]
[66 23 100]	15.1°	—	11.7°	—
[66 $\bar{2}3$ 100]	—	15.1°	—	11.7°
Phosphorescence at 1.77 eV	[94 32 100]	[94 $\bar{3}2$ 100]	[87 34 100]	[87 $\bar{3}4$ 100]
[66 26 100]	14.5°	—	11.5°	—
[66 $\bar{2}6$ 100]	—	14.5°	—	11.5°

were also low intensity broad peaks with highly variable peak energies, typically occurring at around 2.07, 2.48 and 3.76 eV (600, 500 and 330 nm). The authors found the best explanation to be transitions in Fe^{3+} ions at T1 sites on the basis of impurity abundance and theoretical arguments. Individual workers explained minor differences between their peak energies and those obtained by others as being caused by the slightly different crystal fields of the host lattice.

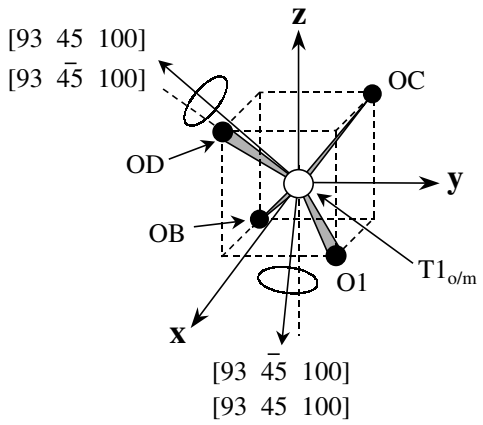

Figure 6. Sketch showing a T1 site in orthoclase and four anions (O1, OB, OC and OD) nearest to it. The tetrahedron is slightly distorted, so the **x**, **y** and **z** directions and each cation–anion direction are only approximate symmetry axes. Two orientations of the four anions can occur; these are tracked by labelling the T1 sites as either $T1_o$ or $T1_m$. The direction of one pair of dipoles deduced from the fits to the 1.77 eV fluorescence data excited with 3.26 eV photons are shown (small arrows). The ellipses represent the experimental error (exaggerated for clarity) in the direction of the dipoles. The way to interpret this figure is as follows. When the tetrahedron is part of the feldspar lattice such that the cation occupies a $T1_o$ site, then the [93 45 100] dipole points close to the direction from the cation to its OD anion, and the [93 $\bar{4}5$ 100] dipole points close to a line from the cation which bisects the angle between its O1 and OB anions (the $-\mathbf{z}$ direction in the figure). When the tetrahedron is in the feldspar lattice such that the cation occupies a $T1_m$ site, the [93 $\bar{4}5$ 100] dipole points close to the direction from the cation to its OD anion, and the [93 45 100] dipole now points close to a line from the cation which bisects the angle between its O1 and OB anions.

No previous excitation spectra using polarized excitation for Fe^{3+} fluorescence are known to exist. However, absorption spectra for polarized light have been presented for feldspars with large iron concentrations and the observed absorption peaks attributed to transitions in Fe^{3+} ions (see Hofmeister and Rossman 1984, White *et al* 1986). Their data show a sharp absorption peak near 3.26 eV and a double peak with maxima around 2.79 and 2.95 eV. Broad, structureless, absorption peaks with low absorption coefficients were also present with absorption maxima at about 2.10 and 2.48 eV. Both papers show the absorption at 2.79 eV appearing only as a shoulder for β polarized light, but as a prominent peak with γ polarized light. The absorption at other energies appeared to be only weakly dependent on the polarization of the incident light. No references were found where the polarization effects in the absorption in feldspars was explained.

The only publication that could be found on the polarization of the 1.77 eV fluorescence from Fe^{3+} ions was by White *et al* (1986), who used 2.61 eV (476 nm) excitation. They found the emission to be strongly polarized, with an intensity that varied by about $\pm 30\%$ from the average.

The excitation spectra using unpolarized excitation of different slices of K3 were very similar to those previously published for Fe^{3+} ions in orthoclase. Although the excitation peaks shown in figure 2 were wider, this was to be expected with the large slit widths employed. It is concluded that these excitation features were clearly due to Fe^{3+} ions in T1 sites of the sample.

The polarization effects in the excitation shown in figures 2 and 3 are partly consistent with the absorption results of other workers in that the 2.79 eV peak only appeared as a shoulder with β polarization, but as a prominent peak with γ polarization. However, the intensity of

the 3.26 eV peak depended significantly on the polarization of the excitation in contrast to the absorption results of Hofmeister and Rossman (1984), or White *et al* (1986). No reasonable explanation can be offered at this time for the discrepancy.

The polarization effects in the emission shown in figures 4 and 5 were similar to the results of White *et al* (1986, their figure 5), although it is difficult to be 100% confident about this because they used a different nomenclature for labelling the principal directions.

The most likely explanation for the observed polarization effects is that the probability of a particular excitation occurring in an Fe^{3+} ion depends on the polarization of the incident photons, and that the emission is polarized.

The excitation of slices A and E with polarized light at 2.79 and 3.26 eV resulted in maxima and minima in the emission intensity when the external polarizer transmission axis was approximately parallel with a principal direction; this is consistent with what one should expect for dipolar transitions. One pair of dipole directions deduced from the data aligned reasonably well with approximate symmetry features of the T1 tetrahedra (table 2). Although dipole directions were deduced for the excitation at 2.92 eV these must be considered as artefacts with no physical meaning since the maximum and minimum in the intensity did not occur when the external polarizer transmission axes aligned with a principal direction. A possible explanation for the latter is that the transitions at 2.92 eV are not dipolar.

When analysing the polarization of the emission, maxima and minima in the intensity also occurred for directions of the external polarizer transmission axis that were consistent with dipolar transitions. That this analysis was independent of the excitation energy (figure 5) is as one would expect for a single emission transition. One pair of dipole directions deduced from the data aligned reasonably well with the same approximate symmetry features of the T1 tetrahedra (table 2) as those deduced from the polarized excitation data, but with larger angles of deviation. This could result from a lattice relaxation occurring when the Fe^{3+} ions are in an excited state.

It is thus concluded that the dipoles deduced from the 1.77, 2.79 and 3.26 eV data are consistent with dipolar transitions in Fe^{3+} ions in T1 sites that have a symmetry axis in the crystal field parallel to one of the deduced dipole directions, but the 2.92 eV transition is not dipolar.

In the next section it will be shown that an analysis of the EPR data of Fe^{3+} ions in microcline feldspars supports the conclusion that the crystal field around Fe^{3+} ions in orthoclase has symmetry axes parallel to the dipole directions deduced from the polarization data.

6. EPR and the crystal field symmetry

It is known from EPR theory that the components of the spectroscopic tensor (g_i) are related to the symmetry axes of a non-cubic crystal field around a paramagnetic ion (Marfunin 1979, p 94). Thus the EPR results of Fe^{3+} cations in microcline given by Marfunin *et al* (1967) allow the direction of the symmetry axes of the crystal field around Fe^{3+} ions in one T1 site, $T1_o$, to be determined[4]. Now since the difference in the microcline and orthoclase lattices is only a slight distortion (Brown and Bailey 1964), the direction of the symmetry axes of crystal field around the $T1_o$ sites in microcline will be practically the same as the T1 sites in orthoclase. Thus if the conclusions of the previous section are correct, one of the axes predicted by the g_i values of microcline should coincide with one of the dipole orientations deduced for the optical transitions for Fe^{3+} ions in orthoclase.

[4] In microcline there are two distinct T1 sites: $T1_o$ and $T1_m$; only information on the $T1_o$ site can be obtained from the EPR data because this site is predominantly occupied by Al^{3+} cations, and thus Fe^{3+} cations will be predominantly found there as well.

The directional cosines given by Marfunin *et al* (1967) for the g_i components were converted into $[u\ \ v\ \ w]$ vectors of the microcline coordinate system given by Brown and Bailey (1964). The three vectors are [95 $\bar{4}$2 100], [$\bar{6}$0 2 100] and [109 156 100]. These vectors are approximately orthogonal to each other, and the [95 $\bar{4}$2 100] vector deviates by less than 10° from the crystal direction $T1_o \longrightarrow (OB + O1)_o$ calculated from x-ray diffraction data for microcline[5]. The other two vectors are close to the directions $OB_o \longrightarrow O1$ and $OC_o \longrightarrow OD_o$ respectively. The [95 $\bar{4}$2 100] vector is almost parallel to the [93 $\bar{4}$5 100] dipole direction deduced from the optical excitation data (the dot product shows that the two vectors deviate by only 2.2°), but deviates considerably from the dipole direction deduced from the 1.77 eV emission data. The latter should be expected since the EPR data are obtained from Fe^{3+} ions which are not in optically excited states where a lattice relaxation may occur. It is thus concluded that the [93 $\bar{4}$5 100] dipole direction aligns with a symmetry axis of a non-cubic crystal field around unexcited Fe^{3+} ions in T1 sites in orthoclase.

A summary of what has been found so far is as follows. The excitation spectra clearly indicated that the 1.77 eV emission was due to Fe^{3+} ions in T1 sites. The polarization effects in the emission, and the 2.79 and 3.26 eV excitation, were consistent with the predictions of a model developed by Short and Huntley (2000). One pair of dipoles deduced from the data for each of these transition energies was closely aligned with two approximate symmetry directions in the average geometry of the four anions around the T1 sites. Finally, EPR data were used to show that the crystal field around an unexcited Fe^{3+} ion has two possible symmetry axes with directions that are very similar to the dipole directions deduced from the optical excitation data. It would thus appear that the method of determining the lattice sites of a defect from the polarization effects in the defect's optical transitions works for Fe^{3+} impurities in orthoclase. The only major assumption not substantiated is that the transitions are dipolar at 1.77, 2.79 and 3.26 eV but not at 2.92 eV; this is investigated in the next section.

7. Determining what transitions in Fe^{3+} ions are dipolar

To determine if an optical transition in an Fe^{3+} ion is dipolar or not, one first needs to ascertain the symmetry in the geometry of its nearest neighbours. Once the symmetry is known one can use group theory to calculate how the optical transition energies are modified from those of the free ion state (Orgel 1955). A positive outcome in this process is achieved if agreement is obtained between the experimental and theoretical transition energies. One can then calculate which transitions are dipolar. The first two steps in this process have been done by a number of workers (see e.g. White *et al* 1986) and therefore all that needs to be done is the final step. However, in all known cases except one, the symmetry used for the second step was that of a regular tetrahedron, for which no polarized transitions can occur, and therefore the results are not relevant. The exception was by Telfer and Walker (1978), who noticed that some excitation peaks began to split into multiple components if data were obtained at low temperatures, and thus realized that the prevailing symmetry was not that of a regular tetrahedron. They instead assumed that the anions around the Fe^{3+} ions were in their average positions[6], and showed that this geometry could qualitatively account for the observed splitting of the weak excitation transition at 2.06 eV (outside the range of our spectra). However, such a symmetry does not

[5] There are two ways to mount a microcline crystal, which results in an ambiguity about which sites are 'o' and which are 'm'. Marfunin *et al* (1967) did not specify their mounting. The assignment of 'o' and 'm' by Bailey and Taylor (1955) was assumed for these alignments. The other possibility results in the [95 $\bar{4}$2 100] vector deviating by less than 10° from parallel with the crystal direction $T1_o \longrightarrow OD_o$.

[6] Anions in average positions do not have axial symmetry, but belong to a lower symmetry class (discussed later).

simultaneously account for the polarization effects in the 2.79 and 3.26 eV transitions presented here, as shall be shown below; thus their proposed symmetry is also rejected and a search for another symmetry that can account for all the data is undertaken.

One approach of ascertaining the symmetry of the crystal field around Fe^{3+} ions in T1 sites is to systematically examine the effect on the optical transitions of all possible arrangements of the four anions. Although there is a large number of ways one can arrange the anions, it turns out that they all fall into one of 11 symmetry groups. The crystal field generated by the geometry of a regular tetrahedron with the cation at the centre belongs to the group with the highest symmetry. A distorted tetrahedron belongs to a group with lower symmetry—which one depends on the type of distortion. For example, by changing the length of one of the anion–cation bonds from a regular tetrahedral geometry, with all bond angles unchanged, one has a crystal field with a threefold rotational axis about this odd bond, and three reflection planes. However, the threefold rotational symmetry axes about the other anion–cation bonds are lost with this distortion as are the twofold rotational axes that coincide with the directions that bisect the angles between any two anion–cation bonds. In this case, the Schönflies symbol for the symmetry group changes from T_d to C_{3v}.

Apart from the T_d group, two others (T and C_1) can be immediately rejected because their symmetries also do not allow polarized transitions to occur. A considerable reduction in the labour of calculating energy diagrams for each of the remaining eight groups is obtained if it is assumed that all the symmetries occur with the anions in positions only slightly displaced from their average ones. In which case transitions in the cation will occur at approximately the same energies for all the symmetry groups, although there may be two or more transitions near one particular energy[7] (see figure 7). Thus one only needs to know what transitions best match the experimental energy values for one symmetry group, to be able to generate the best matches for all the other groups. Once these transitions have been determined for each group, whether they are dipolar or not can be calculated. Using this method three possible symmetry groups lead to dipolar transitions consistent with the excitation results using polarized light and EPR results. However, these same symmetry groups do not predict a dipolar emission process. The details, and a possible explanation, follow.

In table 3 the correlation between transitions for the different symmetry groups and their polarization dependence is given. The task is to identify suitable symmetry groups from the table that can be used to explain the polarization data shown in figure 3. First, one sees that polarized transitions are not allowed at 2.79 eV for the D_{2d} and D_2 groups, but figure 3 shows a clear polarization effect. Second, one sees that there is no differences in the polarization effect for transitions occurring at 2.79 and 2.92 eV for the C_{3v}, C_3 and C_s groups, yet figure 3 shows a clear difference. Thus five out of the eight remaining symmetry groups cannot explain the data and must be rejected, leaving only S_4, C_{2v} and C_2. These three symmetry groups all allow only dipolar transitions with the same polarization near 2.79 and 3.26 eV, but two or more transitions near 2.92 eV with a mixture of different polarizations. This is in qualitative agreement with the polarization data. The three symmetry groups all have axial symmetry with a twofold rotational axis (z), and the dipole associated with the dipolar transitions near 2.79 and 3.26 eV will point along this axis. Furthermore, the z symmetry direction of these three groups will be parallel to either the **x**, **y** or **z** axes shown in figure 6, which is consistent with one of the possible directions deduced from the polarization and EPR data.

Now it must be asked if there is some arrangement of the anions around the Fe^{3+} ions that can be used to explain the polarization of the 1.77 eV emission. First it should be noted

[7] To account for the fact that no structure is observed in the excitation spectra presented here (figure 2) it is assumed that the energy separations were below the resolution of the equipment, or that only one transitions is allowed.

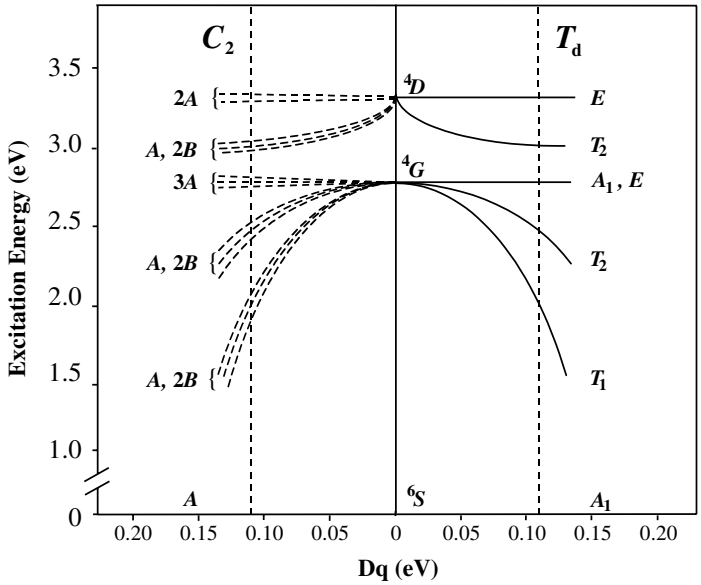

Figure 7. Energy diagrams showing qualitatively how a crystal field with T_d and C_2 symmetries modifies the states of an Fe^{3+} ion. On the centre line are the first three free ion states; the superscripts are their spin multiplicity. Moving along the abscissa in either direction represents introducing the free ion to an electric field, which causes the degeneracy of free ion states to lift. *Dq* is a parameter that depends on the type of cation, the type of anions, and the geometry. The right side of the centre line shows how the states are split for T_d symmetry; this half of the figure is qualitatively the same as that given by White *et al* (1986) for their absorption data, but without the higher energy states. The abscissa is colinear with the ground state which does not split. The vertical dashed line indicates the value of *Dq* at which the transitions from the ground state to the excited states best match the absorption data. A_1, E, T_1 and T_2 are the irreducible representations for the split states. The spin multiplicity of the split states is the same as for the free ion states and has been omitted. The left side of the centre line shows qualitatively how the states are split for C_2 symmetry, assuming that the new geometry occurs because of slight distortion of the bond lengths and/or angles from those of a regular tetrahedron, in which case the energy diagram for the new symmetry can be treated as a perturbation of the old T_d symmetry. A and B are the new irreducible representations for the states in C_2 symmetry obtained from correlation tables.

that no absorption has been observed at 1.77 eV in feldspars despite the strong emission. The explanation for this is that the lattice relaxes[8] before emission, causing the emission photons to have a lower energy than the exciting photons—a 'Stokes shift' (see e.g. Curie 1963, p 31). This is equivalent to moving to higher *Dq* values in the diagram shown in figure 7. White *et al* (1986) claimed that the Stokes shift necessary to cause the lowest energy excitation which is seen at around 2.07 eV (table 3) to shift to 1.77 eV in emission was reasonable. Since the direct products that are used to calculate the polarization effects of a transition commute, and thus they yield the same result for excitation and emission, the entries in table 3 can be used to explain the polarization of the emission (figure 5). However, none of the entries in the last column show a single dipolar transition for any of the symmetry groups; instead, it appears that two or more transitions can occur with a mixture of different polarizations. If this happens, the polarization effect will be smeared out, in contrast to the data shown in figure 5.

A reasonable explanation for this apparent dichotomy is that after excitation the electron rapidly drops to the lowest excited state; thus there is predominantly only one emission

[8] In which case the symmetry need no longer be the same as that prevalent during excitation.

Table 3. Correlation table of transitions for different crystal field symmetries. (Note that the entries in the first column contain symbols for nine symmetry groups that occur for various distortions of a regular tetrahedron. Eight of these groups allow polarized transitions; the T_d group does not, but it is included here for comparison. The symbols in the rows of each symmetry group are the irreducible representations of the modified free ion states. The entries in the T_d row are the transitions from the ground state (A_1) that White *et al* (1986) assigned to their absorption data, and these are in columns whose headings are the approximate energies at which they occur. A Cartesian coordinate below a state signifies the polarization of the excitation photons, calculated from character tables given by Ferraro and Ziomek (1975) and Cotton (1990), required for a transition to occur from the ground state. A single x, y or z means that the transition is dipolar, (x, y) means that the transition occurs with a combination of x and y polarized light, whereas (x), (y) means that the transition can occur with light polarized in either the x or y direction. Note that x, y and z are symmetry directions of the different symmetry groups and are not necessarily parallel with the **x**, **y** and **z** axes shown in figure 6. This table is consistent with that of Bhalla and White (1971). The C_s symmetry group is the group generated by the average geometry of the anions around the T1 sites used by Telfer and Walker (1978).)

Group	3.26 eV (380 nm)	2.92 eV (425 nm)	2.79 eV (445 nm)	2.48 eV (500 nm)	2.06 eV (600 nm)
T_d	$A_1 \rightarrow E$	$A_1 \rightarrow T_2$	$A_1 \rightarrow A_1 + E$	$A_1 \rightarrow T_2$	$A_1 \rightarrow T_1$
D_{2d}	$A_1 \rightarrow A_1 + B_1$	$A_1 \rightarrow \underbrace{B_2}_{(z)} + \underbrace{E}_{(x,y)}$	$A_1 \rightarrow 2A_1 + B_1$	$A_1 \rightarrow \underbrace{B_2}_{(z)} + \underbrace{E}_{(x,y)}$	$A_1 \rightarrow A_2 + \underbrace{E}_{(x,y)}$
C_{3v}	$A_1 \rightarrow \underbrace{E}_{(x,y)}$	$A_1 \rightarrow \underbrace{A_1}_{(z)} + \underbrace{E}_{(x,y)}$	$A_1 \rightarrow \underbrace{A_1}_{(z)} + \underbrace{E}_{(x,y)}$	$A_1 \rightarrow \underbrace{A_1}_{(z)} + \underbrace{E}_{(x,y)}$	$A_1 \rightarrow A_2 + \underbrace{E}_{(x,y)}$
S_4	$A \rightarrow A + \underbrace{B}_{(z)}$	$A \rightarrow \underbrace{B}_{(z)} + \underbrace{E}_{(x,y)}$	$A \rightarrow 2A + \underbrace{B}_{(z)}$	$A \rightarrow \underbrace{B}_{(z)} + \underbrace{E}_{(x,y)}$	$A \rightarrow A + \underbrace{E}_{(x,y)}$
D_2	$A \rightarrow 2A$	$A \rightarrow \underbrace{B_1}_{(z)} + \underbrace{B_2}_{(y)} + \underbrace{B_3}_{(x)}$	$A \rightarrow 3A$	$A \rightarrow \underbrace{B_1}_{(z)} + \underbrace{B_2}_{(y)} + \underbrace{B_3}_{(x)}$	$A \rightarrow \underbrace{B_1}_{(z)} + \underbrace{B_2}_{(y)} + \underbrace{B_3}_{(x)}$
C_{2v}	$A_1 \rightarrow \underbrace{A_1}_{(z)} + A_2$	$A_1 \rightarrow \underbrace{A_1}_{(z)} + \underbrace{B_1}_{(x)} + \underbrace{B_2}_{(y)}$	$A_1 \rightarrow \underbrace{2A_1}_{(z)} + A_2$	$A_1 \rightarrow \underbrace{A_1}_{(z)} + \underbrace{B_1}_{(x)} + \underbrace{B_2}_{(y)}$	$A_1 \rightarrow A_2 + \underbrace{B_1}_{(x)} + \underbrace{B_2}_{(y)}$
C_3	$A \rightarrow \underbrace{E}_{(x,y)}$	$A \rightarrow \underbrace{A}_{(z)} + \underbrace{E}_{(x,y)}$	$A \rightarrow \underbrace{A}_{(z)} + \underbrace{E}_{(x,y)}$	$A \rightarrow \underbrace{A}_{(z)} + \underbrace{E}_{(x,y)}$	$A \rightarrow \underbrace{A}_{(z)} + \underbrace{E}_{(x,y)}$
C_2	$A \rightarrow \underbrace{2A}_{(z)}$	$A \rightarrow \underbrace{A}_{(z)} + \underbrace{2B}_{(x),(y)}$	$A \rightarrow \underbrace{3A}_{(z)}$	$A \rightarrow \underbrace{A}_{(z)} + \underbrace{2B}_{(x),(y)}$	$A \rightarrow \underbrace{A}_{(z)} + \underbrace{2B}_{(x),(y)}$
C_s	$A' \rightarrow \underbrace{A'}_{(x),(y)} + \underbrace{A''}_{(z)}$	$A' \rightarrow \underbrace{2A'}_{(x),(y)} + \underbrace{A''}_{(z)}$	$A' \rightarrow \underbrace{2A'}_{(x),(y)} + \underbrace{A''}_{(z)}$	$A' \rightarrow \underbrace{2A'}_{(x),(y)} + \underbrace{A''}_{(z)}$	$A' \rightarrow \underbrace{A'}_{(x),(y)} + \underbrace{2A''}_{(z)}$

transition and this is dipolar. Telfer and Walker (1978) reached a similar conclusion as they sought to explain why the excitation spectrum near 2.06 eV separated into three peaks at low temperatures, but the emission at 1.77 eV did not. Out of the possible symmetry groups in the last column of table 3, D_2, C_{2v}, C_3, C_2 and C_s all could allow a single dipolar transition to occur. Recall that the dipole direction associated with a dipolar transition will align with a symmetry axis of the crystal field. It has already been mentioned that C_{2v} and C_2 have a twofold symmetry axis (z); D_2 is similar, except that it has three orthogonal twofold symmetry axes (x, y and z) which will be parallel to the **x**, **y** and **z** axes shown in figure 6 but not necessarily in the right order. The C_3 group has one threefold rotational axis (z) which will be parallel to one of the anion–cation bonds, and although the C_s group only has a symmetry plane, its z direction will be parallel to one of the Cartesian axes shown in figure 6. Comparing the dipole directions calculated from group theory with those deduced from the polarization data, one sees that groups D_2, C_3, C_2 and C_s are all viable. The C_{2v} group is rejected because only a x or a y dipole direction is possible, and these are parallel to directions between two anions inconsistent with the two possibilities deduced from the polarization data.

8. Conclusions

It has been shown here that the method proposed by Short (2004) for determining the lattice site of a defect from the polarization effects in an optical transition of the defect correctly predicted the location of Fe^{3+} impurities in orthoclase. The fact that this prediction is supported by EPR analysis and group theory calculations is very encouraging, and gives one greater confidence in the method. However, no explanation could be offered as to why the polarized absorption results of others were not 100% consistent with the fluorescence results presented here. Further tests on other types of defects in orthoclase and similar low symmetry crystals would be beneficial.

Acknowledgments

I would like to thank L Groat for providing me with the K3 orthoclase sample and D J Huntley for assistance with the preparation of this manuscript. This research was supported by a Natural Sciences and Engineering Research Council of Canada (NSERC) grant to DJH.

References

Bailey S W and Taylor W H 1955 The structure of triclinic potassium feldspar *Acta Crystallogr.* **8** 621–32

Bhalla R J R S B and White E W 1971 Intrinsic cathodoluminescence emission from willemite single crystals *J. Lumin.* **4** 194–200

Brown B E and Bailey S W 1964 The structure of maximum microcline *Acta Crystallogr.* **17** 1391–400

Colville A A and Ribbe P H 1968 The crystal structure of an adularia and a refinement of the structure of orthoclase *Am. Mineral.* **53** 25–37

Cotton F A 1990 *Chemical Application of Group Theory* 3rd edn (New York: Wiley)

Curie D 1963 *Luminescence in Crystals* (New York: Wiley)

Deer W A, Howie R A and Zussman J 1992 *An Introduction to the Rock Forming Minerals* 2nd edn (England: Longman)

Ferraro J R and Ziomek J S 1975 *Introductory Group Theory* 2nd edn (New York: Plenum)

Geake J E, Walker G and Telfer D J 1977 The cause and significance of luminescence in lunar plagioclase *Phil. Trans. R. Soc.* A **285** 403–8

Geake J E, Walker G, Telfer D J, Mills A A and Garlick G F J 1973 Luminescence of lunar, terrestrial, and synthesized plagioclase, caused by Mn^{2+} and Fe^{3+} *Proc. 4th Lunar Conf.*; *Geochim. Cosmochim. Acta* **3** (Suppl. 4) 3181–9

Hofmeister A M and Rossman G R 1984 Determination of Fe^{3+} and Fe^{2+} concentrations in feldspar by optical absorption and EPR spectroscopy *Phys. Chem. Mineral.* **11** 213–24

Kirsh Y and Townsend P D 1988 Speculations on the blue and red bands in the TL emission spectrum of albite and microcline *Radiat. Meas.* **14** 43–9

Marfunin A S 1979 *Spectroscopy, Luminescence and Radiation Centers in Minerals* (Berlin: Springer)

Marfunin A S, Bershov L V, Meilman M L and Michoulier J 1967 Paramagnetic resonance of Fe^{3+} in some feldspars *Schweiz. Mineral. Petrogr. Mitt.* **47** 13–20

Nadezhina T N, Pushcharovskii D Yu, Taroev V K, Tauson V L and Bychkov A M 1993 Crystal structure of the ferrialuminosilicate low sanidine *Crystallogr. Rep.* **38** 753–5

Orgel L E 1955 Spectra of transition metal complexes *J. Chem. Phys.* **6** 1004–14

Poolton N R J, Botter Jensen L and Johnsen O 1996 On the relationship between luminescence excitation spectra and feldspar mineralogy *Radiat. Meas.* **26** 93–101

Short M A 2003 An investigation into the physics of the infrared excited luminescence of irradiated feldspars *PhD Thesis* Simon Fraser University, Burnaby, BC Canada, unpublished

Short M A 2004 Determining the possible lattice sites of two unknown defects in orthoclase from the polarization effects in their optical transitions *J. Phys.: Condens. Matter* **16** 7405–17

Short M A and Huntley D J 2000 Crystal anisotropy effects in optically stimulated luminescence of a K-feldspar *Radiat. Meas.* **32** 865–71

Slaats P G, Dirksen G J and Blasse G 1991 Luminescence of some activators in synthetic potassium feldspar crystals *Mater. Chem. Phys.* **30** 19–23

Smith J V and Brown W L 1988 *Feldspar Minerals* 2nd edn, vol 1 (Berlin: Springer)

Telfer D J and Walker G 1975 Optical detection of Fe^{3+} in lunar plagioclase *Nature* **258** 694–5

Telfer D J and Walker G 1978 Ligand field bands of Mn^{2+} and Fe^{3+} luminescence centres and their site occupancy in plagioclase feldspars *Mod. Geol.* **6** 199–210

White W B, Matsumura M, Linnehan D G, Toshiharu F and Chandrasekhar B K 1986 Absorption and luminescence of Fe^{3+} in single-crystal orthoclase *Am. Mineral.* **71** 1415–9

Zink A, Visocekas R and Bos A J J 1995 Comparison of ‘blue’ and ‘infrared’ emission bands in thermoluminescence of alkali feldspars *Radiat. Meas.* **24** 513–8